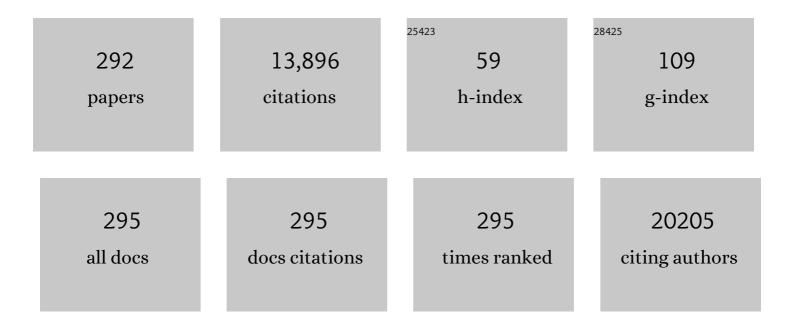
A L Chuvilin

List of Publications by Year in descending order

Source: https://exaly.com/author-pdf/4173225/publications.pdf Version: 2024-02-01



#	Article	IF	CITATIONS
1	Spin Hall Magnetoresistance Effect from a Disordered Interface. ACS Applied Materials & Interfaces, 2022, 14, 8598-8604.	4.0	2
2	Prospects of the multislice method for CBED pattern calculation. International Journal of Materials Research, 2022, 97, 912-919.	0.1	0
3	Double‣attice Packing of Pentagonal Gold Bipyramids in Supercrystals with Triclinic Symmetry. Advanced Materials, 2022, 34, e2200883.	11.1	11
4	Exchange Bias in Molecule/Fe ₃ GeTe ₂ van der Waals Heterostructures via Spinterface Effects. Advanced Materials, 2022, 34, e2200474.	11.1	17
5	Gate-tuneable and chirality-dependent charge-to-spin conversion in tellurium nanowires. Nature Materials, 2022, 21, 526-532.	13.3	62
6	"Missing―One-Dimensional Red-Phosphorus Chains Encapsulated within Single-Walled Carbon Nanotubes. ACS Nano, 2022, 16, 6002-6012.	7.3	14
7	Cucurbit[6]uril as a co-catalyst forÂhydrogen production from formic acid. Materials Today Energy, 2022, 26, 100998.	2.5	4
8	Doping of Carbon Nanotubes with Encapsulated Phosphorus Chains. Inorganic Chemistry, 2022, 61, 9605-9614.	1.9	6
9	Black Au-Decorated TiO ₂ Produced via Laser Ablation in Liquid. ACS Applied Materials & Interfaces, 2021, 13, 6522-6531.	4.0	32
10	Coupling plasmonic catalysis and nanocrystal growth through cyclic regeneration of NADH. Nanoscale, 2021, 13, 15188-15192.	2.8	2
11	Structure and Formation Kinetics of Millimeter‣ize Single Domain Supercrystals. Advanced Functional Materials, 2021, 31, 2101869.	7.8	9
12	In-SEM micro-machining reveals the origins of the size effect in the cutting energy. Scientific Reports, 2021, 11, 2088.	1.6	6
13	Paramagnetic spin Hall magnetoresistance. Physical Review B, 2021, 104, .	1.1	18
14	Large spin-charge interconversion induced by interfacial spin-orbit coupling in a highly conducting all-metallic system. Physical Review B, 2021, 104, .	1.1	9
15	Strong Interfacial Exchange Field in a Heavy Metal/Ferromagnetic Insulator System Determined by Spin Hall Magnetoresistance. Nano Letters, 2020, 20, 6815-6823.	4.5	22
16	Particle atomic layer deposition as an effective way to enhance Li-S battery energy density. Materials Today Energy, 2020, 18, 100567.	2.5	4
17	Probing Chemical Kinetics in Two Dimensional Materials Using Atomic Resolution Imaging Microscopy and Microanalysis, 2020, 26, 90-90.	0.2	0
18	Strain-induced structure and oxygen transport interactions in epitaxial La0.6Sr0.4CoO3â~î´ thin films. Communications Materials, 2020, 1, .	2.9	8

#	Article	IF	CITATIONS
19	Beneficial role of the nitrogen-doped carbon nanotubes in the synthesis of the active palladium supported catalyst. Diamond and Related Materials, 2019, 98, 107484.	1.8	11
20	Coupling HAADF-STEM Tomography and Image Reconstruction for the Precise Characterization of Particle Morphology of Composite Polymer Latexes. Macromolecules, 2019, 52, 5298-5306.	2.2	17
21	Ionic liquid-based electrodeposition of ZnS:nano-MoS2 composite films with self-lubricating properties. Surface and Coatings Technology, 2019, 374, 957-965.	2.2	8
22	Spin Hall magnetoresistance in a low-dimensional Heisenberg ferromagnet. Physical Review B, 2019, 100, .	1.1	21
23	Large Multidirectional Spin-to-Charge Conversion in Low-Symmetry Semimetal MoTe ₂ at Room Temperature. Nano Letters, 2019, 19, 8758-8766.	4.5	81
24	Impact of Symmetry on Anisotropic Magnetoresistance in Textured Ferromagnetic Thin Films. Physical Review Letters, 2019, 123, 137201.	2.9	22
25	Ligand-induced reduction concerted with coating by atomic layer deposition on the example of TiO ₂ -coated magnetite nanoparticles. Chemical Science, 2019, 10, 2171-2178.	3.7	11
26	Hydrogen Production from Formic Acid over Au Catalysts Supported on Carbon: Comparison with Au Catalysts Supported on SiO2 and Al2O3. Catalysts, 2019, 9, 376.	1.6	24
27	Films of filled single-wall carbon nanotubes as a new material for high-performance air-sustainable transparent conductive electrodes operating in a wide spectral range. Nanoscale, 2019, 11, 6755-6765.	2.8	17
28	Holey graphene with enhanced near-infrared absorption: Experimental and DFT study. Applied Physics Letters, 2019, 114, .	1.5	9
29	The Route to Supercurrent Transparent Ferromagnetic Barriers in Superconducting Matrix. ACS Nano, 2019, 13, 5655-5661.	7.3	4
30	Single Au Atoms on the Surface of N-Free and N-Doped Carbon: Interaction with Formic Acid and Methanol Molecules. Topics in Catalysis, 2019, 62, 508-517.	1.3	19
31	Design of Intense Nanoscale Stray Fields and Gradients at Magnetic Nanorod Interfaces. ACS Applied Materials & Interfaces, 2019, 11, 4678-4685.	4.0	8
32	Investigation of the exceptional charge performance of the 0.93Li4â^'xMn2O5–0.07Li2O composite cathode for Li-ion batteries. Journal of Materials Chemistry A, 2018, 6, 5156-5165.	5.2	18
33	Origin of large plasticity and multiscale effects in iron-based metallic glasses. Nature Communications, 2018, 9, 1333.	5.8	89
34	Creation of nanosized holes in graphene planes for improvement of rate capability of lithium-ion batteries. Nanotechnology, 2018, 29, 134001.	1.3	40
35	Co-Solvent Effect in the Processing of the Perovskite:Fullerene Blend Films for Electron Transport Layer-Free Solar Cells. Journal of Physical Chemistry C, 2018, 122, 2512-2520.	1.5	19
36	Bifunctional Oxygen Reduction/Oxygen Evolution Activity of Mixed Fe/Co Oxide Nanoparticles with Variable Fe/Co Ratios Supported on Multiwalled Carbon Nanotubes. ChemSusChem, 2018, 11, 1204-1214.	3.6	49

#	Article	IF	CITATIONS
37	Submicron pillars of ferromagnetic shape memory alloys: Thermomechanical behavior. Applied Materials Today, 2018, 12, 9-14.	2.3	6
38	Optimization of monochromated TEM for ultimate resolution imaging and ultrahigh resolution electron energy loss spectroscopy. Ultramicroscopy, 2018, 184, 109-115.	0.8	30
39	Fe–Mo and Co–Mo Catalysts with Varying Composition for Multiâ€Walled Carbon Nanotube Growth. Physica Status Solidi (B): Basic Research, 2018, 255, 1700260.	0.7	26
40	Effect of Hydrogen Fluoride Addition and Synthesis Temperature on the Structure of Doubleâ€Walled Carbon Nanotubes Fluorinated by Molecular Fluorine. Physica Status Solidi (B): Basic Research, 2018, 255, 1700261.	0.7	4
41	TEM Study of Current-Induced Domain Wall Motion in Cylindrical Nanowires: Towards 3D Magnetic Memory Devices. Microscopy and Microanalysis, 2018, 24, 944-945.	0.2	2
42	Synthetic Antiferromagnetic Coupling Between Ultrathin Insulating Garnets. Physical Review Applied, 2018, 10, .	1.5	34
43	Highly Stable Singleâ€Atom Catalyst with Ionic Pd Active Sites Supported on Nâ€Doped Carbon Nanotubes for Formic Acid Decomposition. ChemSusChem, 2018, 11, 3724-3727.	3.6	99
44	Microstructural aspects of the transition between two regimes in orthogonal cutting of AISI 1045 steel. Journal of Materials Processing Technology, 2018, 260, 87-96.	3.1	12
45	Nanoporous thin films obtained by oblique angle deposition of aluminum on porous surfaces. Surface and Coatings Technology, 2018, 347, 350-357.	2.2	7
46	Effect of in-plane size of MoS2 nanoparticles grown over multilayer graphene on the electrochemical performance of anodes in Li-ion batteries. Electrochimica Acta, 2018, 283, 45-53.	2.6	17
47	Understanding the Image Contrast of Material Boundaries in IR Nanoscopy Reaching 5 nm Spatial Resolution. ACS Photonics, 2018, 5, 3372-3378.	3.2	69
48	Colloidal branched CdSe/CdS â€~nanospiders' with 2D/1D heterostructure. Nanotechnology, 2018, 29, 395604.	1.3	3
49	Addressing Vibrational Excitations in Van der Waals Materials and Molecular Layers Within Electron Energy Loss Spectroscopy. Microscopy and Microanalysis, 2018, 24, 408-409.	0.2	0
50	Unveiling the mechanisms of the spin Hall effect in Ta. Physical Review B, 2018, 98, .	1.1	56
51	Large-Scale Plasmonic Pyramidal Supercrystals via Templated Self-Assembly of Monodisperse Gold Nanospheres. Journal of Physical Chemistry C, 2017, 121, 10899-10906.	1.5	78
52	An approach to growth of Fe–Si multilayers with controlled composition profile—a way to exchange coupled thin films. Nanotechnology, 2017, 28, 115303.	1.3	5
53	Saturable absorption in detonation nanodiamond dispersions. Journal of Nanophotonics, 2017, 11, 032506.	0.4	6
54	Direct Observation of Current-Induced Motion of a 3D Vortex Domain Wall in Cylindrical Nanowires. ACS Applied Materials & Interfaces, 2017, 9, 16741-16744.	4.0	21

#	Article	IF	CITATIONS
55	Photoinduced effects in field electron emission from diamond needles. Applied Physics Letters, 2017, 110, .	1.5	14
56	Copper on carbon materials: stabilization by nitrogen doping. Journal of Materials Chemistry A, 2017, 5, 10574-10583.	5.2	103
57	Size effect and scaling power-law for superelasticity in shape-memory alloys at the nanoscale. Nature Nanotechnology, 2017, 12, 790-796.	15.6	70
58	Factors Influencing the Performance of Pd/C Catalysts in the Green Production of Hydrogen from Formic Acid. ChemSusChem, 2017, 10, 720-730.	3.6	76
59	Cobalt oxide as a selective co-catalyst for water oxidation in the presence of an organic dye. Photochemical and Photobiological Sciences, 2017, 16, 1771-1777.	1.6	2
60	The growth of new extended carbon nanophases from ferrocene inside singleâ€walled carbon nanotubes. Physica Status Solidi - Rapid Research Letters, 2017, 11, 1700158.	1.2	17
61	Probing low-energy hyperbolic polaritons in van der Waals crystals with an electron microscope. Nature Communications, 2017, 8, 95.	5.8	111
62	Single-Walled Carbon Nanotube Reactor for Redox Transformation of Mercury Dichloride. ACS Nano, 2017, 11, 8643-8649.	7.3	38
63	Design of active and stable oxygen reduction reaction catalysts by embedding Co x O y nanoparticles into nitrogen-doped carbon. Nano Research, 2017, 10, 97-107.	5.8	25
64	Laser-triggered proton acceleration from hydrogenated low-density targets. Physical Review Accelerators and Beams, 2017, 20, .	0.6	11
65	Active Morphology Control for Concomitant Long Distance Spin Transport and Photoresponse in a Single Organic Device. Advanced Materials, 2016, 28, 2609-2615.	11.1	77
66	Field emission from single-walled carbon nanotubes modified by annealing and CuCl doping. Applied Physics Letters, 2016, 109, .	1.5	5
67	Periodic Magnetization Pattern for Controlled Domain Wall Motion in Nanowires. Microscopy and Microanalysis, 2016, 22, 1678-1679.	0.2	1
68	Single crystalline cylindrical nanowires – toward dense 3D arrays of magnetic vortices. Scientific Reports, 2016, 6, 23844.	1.6	45
69	Carbon microspheres preparation, graphitization and surface functionalization for glycerol etherification. Catalysis Today, 2016, 277, 68-77.	2.2	27
70	Support effect for nanosized Au catalysts in hydrogen production from formic acid decomposition. Catalysis Science and Technology, 2016, 6, 6853-6860.	2.1	56
71	Reaction kinetics of bond rotations in graphene. Carbon, 2016, 105, 176-182.	5.4	18
72	Modulated Magnetic Nanowires for Controlling Domain Wall Motion: Toward 3D Magnetic Memories. ACS Nano, 2016, 10, 5326-5332.	7.3	126

#	Article	IF	CITATIONS
73	Virus-Templated Near-Amorphous Iron Oxide Nanotubes. Langmuir, 2016, 32, 5899-5908.	1.6	16
74	Enhanced supercapacitance of vertically aligned multiâ€wall carbon nanotube array covered by MoS ₂ nanoparticles. Physica Status Solidi (B): Basic Research, 2016, 253, 2451-2456.	0.7	11
75	Optical properties and charge transfer effects in single-walled carbon nanotubes filled with functionalized adamantane molecules. Carbon, 2016, 109, 87-97.	5.4	15
76	Photocatalytic and magnetic titanium dioxide/polystyrene/magnetite composite hybrid polymer particles. Journal of Polymer Science Part A, 2016, 54, 3350-3356.	2.5	12
77	Microstructural Changes in La1â^'xCaxCoO3â^'Î^ Solid Solutions Under the Influence of Catalytic Reaction of Methane Combustion. Topics in Catalysis, 2016, 59, 1354-1360.	1.3	4
78	Electron Transport Layerâ€Free Solar Cells Based on Perovskite–Fullerene Blend Films with Enhanced Performance and Stability. ChemSusChem, 2016, 9, 2679-2685.	3.6	60
79	Tunable magnetic nanowires for biomedical and harsh environment applications. Scientific Reports, 2016, 6, 24189.	1.6	88
80	Structural peculiarities of single crystal diamond needles of nanometer thickness. Nanotechnology, 2016, 27, 455707.	1.3	12
81	In-Situ Study of Domain Walls Propagation and Pinning in Modulated Magnetic Nanowires Microscopy and Microanalysis, 2016, 22, 832-833.	0.2	1
82	Remote Magnetomechanical Nanoactuation. Small, 2016, 12, 1013-1023.	5.2	44
83	Single Isolated Pd ²⁺ Cations Supported on N-Doped Carbon as Active Sites for Hydrogen Production from Formic Acid Decomposition. ACS Catalysis, 2016, 6, 681-691.	5.5	252
84	Plasmonic substrates comprising gold nanostars efficiently regenerate cofactor molecules. Journal of Materials Chemistry A, 2016, 4, 7045-7052.	5.2	30
85	Hierarchical organization and molecular diffusion in gold nanorod/silica supercrystal nanocomposites. Nanoscale, 2016, 8, 7914-7922.	2.8	35
86	Multiscale differential phase contrast analysis with a unitary detector. Ultramicroscopy, 2016, 162, 74-81.	0.8	20
87	Temperature dependent radiative and non-radiative recombination dynamics in CdSe–CdTe and CdTe–CdSe type II hetero nanoplatelets. Physical Chemistry Chemical Physics, 2016, 18, 3197-3203.	1.3	41
88	Ferromagnetics: Weak Delocalization in Graphene on a Ferromagnetic Insulating Film (Small 47/2015). Small, 2015, 11, 6242-6242.	5.2	1
89	Weak Delocalization in Graphene on a Ferromagnetic Insulating Film. Small, 2015, 11, 6295-6301.	5.2	7
90	Effect of alkali-soluble resin emulsifiers on coalescence and interdiffusion between latex polymer particles. Colloid and Polymer Science, 2015, 293, 2419-2427.	1.0	11

#	Article	IF	CITATIONS
91	Conjugated Polymers As Molecular Gates for Light-Controlled Release of Gold Nanoparticles. ACS Applied Materials & Interfaces, 2015, 7, 15692-15695.	4.0	7
92	Electron microscopy of single-wall carbon nanotubes-polymer-Pt(Ru) composite materials. Journal of Surface Investigation, 2015, 9, 355-363.	0.1	1
93	Colloidal synthesis and optical properties of type-II CdSe–CdTe and inverted CdTe–CdSe core–wing heteronanoplatelets. Nanoscale, 2015, 7, 8084-8092.	2.8	54
94	Segregation of materials in double precursor electron-beam-induced-deposition: a route to functional magnetic nanostructures. Nanotechnology, 2015, 26, 375302.	1.3	4
95	On the variation of magnetic anisotropy in Co/Pt(111) on silicon oxide. Journal of Applied Physics, 2015, 117, .	1.1	21
96	Functionalization of Defect Sites in Graphene with RuO ₂ for High Capacitive Performance. ACS Applied Materials & Interfaces, 2015, 7, 20513-20519.	4.0	36
97	Plasmon-driven photoregeneration of cofactor molecules. Chemical Communications, 2015, 51, 5330-5333.	2.2	30
98	Chiral templating of self-assembling nanostructures by circularly polarized light. Nature Materials, 2015, 14, 66-72.	13.3	330
99	In Situ Monitoring of DNAâ€Aptavalve Gating Function on Mesoporous Silica Nanoparticles. Particle and Particle Systems Characterization, 2014, 31, 161-167.	1.2	19
100	Crystallographically driven magnetic behaviour of arrays of monocrystalline Co nanowires. Nanotechnology, 2014, 25, 475702.	1.3	51
101	Gold Spiky Nanodumbbells: Anisotropy in Gold Nanostars. Particle and Particle Systems Characterization, 2014, 31, 77-80.	1.2	20
102	Electron microscopy study of a Pt-Pd bimetallic structure formation on soot for catalytic systems. Nanotechnologies in Russia, 2014, 9, 485-491.	0.7	3
103	Polarization-Resolved Near-Field Characterization of Nanoscale Infrared Modes in Transmission Lines Fabricated by Gallium and Helium Ion Beam Milling. ACS Photonics, 2014, 1, 604-611.	3.2	11
104	Linear and non-linear optical properties of filled single-wall carbon nanotubes. , 2014, , .		0
105	Nanometer-Sized MoS ₂ Clusters on Graphene Flakes for Catalytic Formic Acid Decomposition. ACS Catalysis, 2014, 4, 3950-3956.	5.5	49
106	Optical properties of singleâ€walled carbon nanotubes filled with CuCl by gasâ€phase technique. Physica Status Solidi (B): Basic Research, 2014, 251, 2466-2470.	0.7	36
107	Recovery of Permittivity and Depth from Near-Field Data as a Step toward Infrared Nanotomography. ACS Nano, 2014, 8, 6911-6921.	7.3	91
108	FEBID fabrication and magnetic characterization of individual nano-scale and micro-scale Co structures. Nanofabrication, 2014, 1, .	1.1	8

#	Article	IF	CITATIONS
109	Magnetic structure of a single-crystal hcp electrodeposited cobalt nanowire. Europhysics Letters, 2013, 102, 17009.	0.7	45
110	Room-temperature air-stable spin transport in bathocuproine-based spin valves. Nature Communications, 2013, 4, .	5.8	74
111	CdSe–CdS Nanoheteroplatelets with Efficient Photoexcitation of Central CdSe Region through Epitaxially Grown CdS Wings. Journal of the American Chemical Society, 2013, 135, 14476-14479.	6.6	103
112	Knock-on damage in bilayer graphene: Indications for a catalytic pathway. Physical Review B, 2013, 88, .	1.1	19
113	Ultradisperse catalytic layers supported by nanotubes and poly(diallyldimethylammonium)chloride polymer. Russian Journal of Electrochemistry, 2013, 49, 265-271.	0.3	5
114	Ultrathin rechargeable all-solid-state batteries based on monolayer graphene. Journal of Materials Chemistry A, 2013, 1, 3177.	5.2	60
115	Inclusion of radiation damage dynamics in high-resolution transmission electron microscopy image simulations: The example of graphene. Physical Review B, 2013, 87, .	1.1	31
116	Resonant Antenna Probes for Tip-Enhanced Infrared Near-Field Microscopy. Nano Letters, 2013, 13, 1065-1072.	4.5	114
117	The Condensation of Water on Adsorbed Viruses Langmuir, 2013, 29, 14580-14587.	1.6	12
118	Origin and control of magnetic exchange coupling in between focused electron beam deposited cobalt nanostructures. Applied Physics Letters, 2013, 103, .	1.5	20
119	Interfacial and Network Characteristics of Silicon Nanoparticle Layers Used in Printed Electronics. Japanese Journal of Applied Physics, 2013, 52, 05DA11.	0.8	8
120	The Mechanism of {113} Defect Formation in Silicon: Clustering of Interstitial–Vacancy Pairs Studied by <i>In Situ</i> High-Resolution Electron Microscope Irradiation. Microscopy and Microanalysis, 2013, 19, 38-42.	0.2	14
121	The structure and electronic properties of copper iodide 1D nanocrystals within single walled carbon nanotubes. Journal of Physics: Conference Series, 2013, 471, 012035.	0.3	3
122	Enhanced resolution in subsurface near-field optical microscopy. Optics Express, 2012, 20, 593.	1.7	63
123	Quantitative Analysis of Electron Beam-Induced Destruction of Graphene Membranes under an Electron Microscope. Microscopy and Microanalysis, 2012, 18, 1500-1501.	0.2	0
124	Crystallography-Driven Positive Exchange Bias in <mml:math xmlns:mml="http://www.w3.org/1998/Math/MathML" display="inline"><mml:mi>Co</mml:mi><mml:mo>/</mml:mo><mml:mi>CoO</mml:mi>Bilayers. Physical Review Letters, 2012, 109, 177205.</mml:math 	2.9	42
125	Enhancement effects in plasmonic nanocavities with quantum emitters. , 2012, , .		0
126	Correlative infrared–electron nanoscopy reveals the local structure–conductivity relationship in zinc oxide nanowires. Nature Communications, 2012, 3, 1131.	5.8	53

#	Article	IF	CITATIONS
127	Determination of the Coalescence Temperature of Latexes by Environmental Scanning Electron Microscopy. ACS Applied Materials & Interfaces, 2012, 4, 4276-4282.	4.0	21
128	Whispering gallery modes microcavities with J-aggregates and plasmonic hot spots. Proceedings of SPIE, 2012, , .	0.8	0
129	Size, Structure, and Helical Twist of Graphene Nanoribbons Controlled by Confinement in Carbon Nanotubes. ACS Nano, 2012, 6, 3943-3953.	7.3	134
130	Accurate Measurement of Electron Beam Induced Displacement Cross Sections for Single-Layer Graphene. Physical Review Letters, 2012, 108, 196102.	2.9	383
131	Magneto-optical magnetometry of individual 30 nm cobalt nanowires grown by electron beam induced deposition. Applied Physics Letters, 2012, 100, 142401.	1.5	50
132	The structure of 1D and 3D CuI nanocrystals grown within 1.5–2.5 nm single wall carbon nanotubes obtained by catalyzed chemical vapor deposition. Carbon, 2012, 50, 4696-4704.	5.4	30
133	Optical and structural properties of Nb2O5–SiO2 mixtures in thin films. Surface and Coatings Technology, 2012, 206, 3650-3657.	2.2	11
134	Functionalised endohedral fullerenes in single-walled carbon nanotubes. Chemical Communications, 2011, 47, 2116-2118.	2.2	45
135	Whispering gallery mode resonators with J-aggregates. Optics Express, 2011, 19, 22280.	1.7	32
136	Experimental analysis of charge redistribution dueÂto chemical bonding by high-resolution transmission electron microscopy. Nature Materials, 2011, 10, 209-215.	13.3	270
137	Nanofocusing of mid-infrared energy with tapered transmission lines. Nature Photonics, 2011, 5, 283-287.	15.6	203
138	Self-assembly of a sulphur-terminated graphene nanoribbon within a single-walled carbon nanotube. Nature Materials, 2011, 10, 687-692.	13.3	253
139	Transmission electron microscopy study of the microstructure of amorphous Co-P alloy films on various spatial scales. Russian Metallurgy (Metally), 2011, 2011, 465-470.	0.1	5
140	Threeâ€dimensional GaN for semipolar light emitters. Physica Status Solidi (B): Basic Research, 2011, 248, 549-560.	0.7	62
141	Biodegradable Polymeric Nanoparticles as Templates for Biomimetic Mineralization of Calcium Phosphate. Macromolecular Chemistry and Physics, 2011, 212, 915-925.	1.1	13
142	Mid-infrared nanophotonics based on antennas and transmission lines. , 2011, , .		0
143	Effect of internal strain fields on the controllability of nanodimensional ferroelectric films in a plane capacitor. Technical Physics, 2010, 55, 395-399.	0.2	2
144	Synthesis and properties of hydroxyapatite-containing porous titania coating on ultrafine-grained titanium by micro-arc oxidation. Acta Biomaterialia, 2010, 6, 2816-2825.	4.1	171

#	Article	IF	CITATIONS
145	Grain refinement and mechanical properties in ultrafine grained Pd and Pd–Ag alloys produced by HPT. Materials Science & Engineering A: Structural Materials: Properties, Microstructure and Processing, 2010, 527, 1776-1783.	2.6	41
146	Beobachtung chemischer Reaktionen auf atomarer Ebene: Dynamik von Fullerenverschmelzung und NanorĶhrenbruch durch Vermittlung von Metallionen. Angewandte Chemie, 2010, 122, 197-201.	1.6	9
147	Observations of Chemical Reactions at the Atomic Scale: Dynamics of Metalâ€Mediated Fullerene Coalescence and Nanotube Rupture. Angewandte Chemie - International Edition, 2010, 49, 193-196.	7.2	52
148	Mechanical behaviour and in situ observation of shear bands in ultrafine grained Pd and Pd–Ag alloys. Acta Materialia, 2010, 58, 967-978.	3.8	43
149	Accessing the local three-dimensional structure of carbon materials sensitive to an electron beam. Carbon, 2010, 48, 4042-4048.	5.4	11
150	GalnNâ€based LED structures on selectively grown semiâ€polar crystal facets. Physica Status Solidi (A) Applications and Materials Science, 2010, 207, 1407-1413.	0.8	22
151	Topology peculiarities of graphite films of nanometer thickness. Physica Status Solidi (B): Basic Research, 2010, 247, 3010-3013.	0.7	12
152	Thermal oxidation of lattice matched InAlN/GaN heterostructures. Physica Status Solidi C: Current Topics in Solid State Physics, 2010, 7, 13-16.	0.8	13
153	Semipolar GaInN/GaN lightâ€emitting diodes grown on honeycomb patterned substrates. Physica Status Solidi C: Current Topics in Solid State Physics, 2010, 7, 2140-2143.	0.8	27
154	Direct transformation of graphene to fullerene. Nature Chemistry, 2010, 2, 450-453.	6.6	361
155	Influence of nano-oxide layer on the giant magnetoresistance and exchange bias of NiMn/Co/Cu/Co spin valve sensors. Journal of Applied Physics, 2010, 107, 093910.	1.1	5
156	Testing the Temperature Limits of GaN-Based HEMT Devices. IEEE Transactions on Device and Materials Reliability, 2010, 10, 427-436.	1.5	115
157	Stability of Fluorinated Double-Walled Carbon Nanotubes Produced by Different Fluorination Techniques. Chemistry of Materials, 2010, 22, 4197-4203.	3.2	49
158	Atomic Structure of Reduced Graphene Oxide. Nano Letters, 2010, 10, 1144-1148.	4.5	1,076
159	Highly dense amorphous Nb2O5 films with closed nanosized pores. Applied Physics Letters, 2009, 95, 081904.	1.5	15
160	Oxygen induced strain field homogenization in AlN nucleation layers and its impact on GaN grown by metal organic vapor phase epitaxy on sapphire: An x-ray diffraction study. Journal of Applied Physics, 2009, 105, .	1.1	39
161	FePt Nanorods and Nanowires for Novel Ferrofluids. Solid State Phenomena, 2009, 154, 89-94.	0.3	1
162	Reliability behavior of GaN HEMTs related to Au diffusion at the Schottky interface. Physica Status Solidi C: Current Topics in Solid State Physics, 2009, 6, S976.	0.8	38

#	Article	IF	CITATIONS
163	Epitaxial and polycrystalline CuInS2 layers: Structural metastability and its influence on the photoluminescence. Thin Solid Films, 2009, 517, 2248-2251.	0.8	14
164	The correlation between mechanical stress, thermal shift and refractive index in HfO2, Nb2O5, Ta2O5 and SiO2 layers and its relation to the layer porosity. Thin Solid Films, 2009, 517, 6058-6068.	0.8	71
165	Chiral carbon nanoscrolls with a polygonal cross-section. Carbon, 2009, 47, 3099-3105.	5.4	37
166	High-resolution transmission electron microscopy of heteroepitaxial barium strontium titanate films grown on MgO substrates. Journal of Surface Investigation, 2009, 3, 542-547.	0.1	1
167	Exterior surface damage of calcium fluoride outcoupling mirrors for DUV lasers. Optics Express, 2009, 17, 8253.	1.7	10
168	Production of single crystal diamond needles by a combination of CVD growth and thermal oxidation. Diamond and Related Materials, 2009, 18, 1289-1293.	1.8	46
169	InAlN/GaN MOSHEMT With Self-Aligned Thermally Generated Oxide Recess. IEEE Electron Device Letters, 2009, 30, 1131-1133.	2.2	59
170	Depletion of surface accumulation charge in InN by anodic oxidation. Journal of Applied Physics, 2009, 105, 033702.	1.1	18
171	Electron Microscopic Studies with Graphene. Microscopy and Microanalysis, 2009, 15, 126-127.	0.2	5
172	From graphene constrictions to single carbon chains. New Journal of Physics, 2009, 11, 083019.	1.2	280
173	Above 500 °C operation of InAlN/GaN HEMTs. , 2009, , .		3
174	Selective Sputtering and Atomic Resolution Imaging of Atomically Thin Boron Nitride Membranes. Nano Letters, 2009, 9, 2683-2689.	4.5	488
175	Characterization of grain structure in nanocrystalline gadolinium by high-resolution transmission electron microscopy. Journal of Materials Research, 2009, 24, 342-346.	1.2	21
176	Investigation of the Microstructure of Co/Cu/Co/NiMn Spin Valve Systems. Science of Advanced Materials, 2009, 1, 198-204.	0.1	2
177	Detonation synthesis nanodiamonds for reinforcing metal matrix composite coatings operated under shock load. , 2009, , .		0
178	Bluishâ€green semipolar GaInN/GaN light emitting diodes on {1\$ ar 1 \$01} GaN side facets. Physica Status Solidi C: Current Topics in Solid State Physics, 2008, 5, 2059-2062.	0.8	7
179	Transport properties in n-type AlGaN/AlN/GaN-superlattices. Physica Status Solidi C: Current Topics in Solid State Physics, 2008, 5, 1950-1952.	0.8	5
180	Fabrication of radial superlattices based on different hybrid materials. Physica Status Solidi C: Current Topics in Solid State Physics, 2008, 5, 2704-2708.	0.8	19

#	Article	IF	CITATIONS
181	Biomimetic Hydroxyapatite Crystallization in Gelatin Nanoparticles Synthesized Using a Miniemulsion Process. Advanced Functional Materials, 2008, 18, 2221-2227.	7.8	76
182	Process optimization for the effective reduction of threading dislocations in MOVPE grown GaN using in situ deposited masks. Journal of Crystal Growth, 2008, 310, 4867-4870.	0.7	67
183	Quantification and Segmentation of Electron Tomography Data- Exemplified at ErSi2 Nanocrystals in SiC. , 2008, , 321-322.		0
184	Optical and structural properties of LaF_3 thin films. Applied Optics, 2008, 47, C157.	2.1	18
185	Optimization of semipolar GalnN/GaN blue/green light emitting diode structures on {1-101} GaN side facets. , 2008, , .		7
186	Evaluation of Frozen Phonons Models for Multislice Calculation of TDS. Microscopy and Microanalysis, 2007, 13, 130-131.	0.2	8
187	Investigating the Oxide Barrier Layer in Ta-Co-Cu-Co/Oxide/Co-NiMn Spin Valve Structures Microscopy and Microanalysis, 2007, 13, 404-405.	0.2	Ο
188	Electron Tomographic Characterization of Er doped SiC. Microscopy and Microanalysis, 2007, 13, 116-117.	0.2	1
189	The Stability of High Tension Measured by Convergent Beam Electron Diffraction as Base for High Accuracy of Lattice Parameter Determination. Microscopy and Microanalysis, 2007, 13, 132-133.	0.2	0
190	Barrier layer downscaling of InAIN/GaN HEMTs. Device Research Conference, IEEE Annual, 2007, , .	0.0	8
191	Deactivation of a Au/CeO2 catalyst during the low-temperature water–gas shift reaction and its reactivation: A combined TEM, XRD, XPS, DRIFTS, and activity study. Journal of Catalysis, 2007, 250, 139-150.	3.1	114
192	Structural and spectroscopic properties of AlN layers grown by MOVPE. Journal of Crystal Growth, 2007, 298, 383-386.	0.7	19
193	Application of high-resolution electron microscopy for visualization and quantitative analysis of strain fields in heterostructures. Bulletin of the Russian Academy of Sciences: Physics, 2007, 71, 1426-1432.	0.1	38
194	Influence of the catalyst surface area on the activity and stability of Au/CeO2 catalysts for the low-temperature water gas shift reaction. Topics in Catalysis, 2007, 44, 183-198.	1.3	53
195	Investigation of the formation process of nanosized particles of Ru(III). Journal of Structural Chemistry, 2007, 48, 144-149.	0.3	5
196	Prospects of the multislice method for CBED pattern calculation. International Journal of Materials Research, 2006, 97, 912-919.	0.1	2
197	Thermal effects in Raman spectra of hexagonal boron nitride and nanotube-containing boron nitride soot. Physica Status Solidi (B): Basic Research, 2006, 243, 3316-3319.	0.7	13
198	Electron microtomography: A new method for studying the spatial structure of catalysts. Kinetics and Catalysis, 2006, 47, 464-466.	0.3	4

#	Article	IF	CITATIONS
199	Catalytic filamentous carbons-supported Ni for low-temperature methane decomposition. Catalysis Today, 2005, 102-103, 115-120.	2.2	36
200	Orientational effect of the texture of a carbon-nanotube film on CKα a radiation intensity. JETP Letters, 2005, 81, 34-38.	0.4	19
201	Synthesis, characterization and catalytic application for wet oxidation of phenol of iron-containing clays. Applied Catalysis B: Environmental, 2005, 59, 243-248.	10.8	83
202	Electronic state of nanodiamond/graphite interfaces. Applied Physics A: Materials Science and Processing, 2005, 81, 393-398.	1.1	8
203	On the peculiarities of CBED pattern formation revealed by multislice simulation. Ultramicroscopy, 2005, 104, 73-82.	0.8	57
204	On the origin of HOLZ lines splitting near interfaces: multislice simulation of CBED patterns. Journal of Electron Microscopy, 2005, 54, 515-517.	0.9	20
205	Comparison of Structure and Conductivity of Multiwall Carbon Nanotubes Obtained over Ni and Ni/Fe Catalysts. Fullerenes Nanotubes and Carbon Nanostructures, 2005, 12, 93-97.	1.0	8
206	On the mechanism of {113}-defect formation in Si. , 2005, , 359-362.		6
207	The effect of the signal-to-noise ratio in CBED patterns on the accuracy of lattice parameter determination. Journal of Electron Microscopy, 2004, 53, 237-244.	0.9	8
208	Coprecipitated iron-containing catalysts (Fe-Al2O3, Fe-Co-Al2O3, Fe-Ni-Al2O3) for methane decomposition at moderate temperatures. Applied Catalysis A: General, 2004, 270, 87-99.	2.2	83
209	Carbon redistribution processes in nanocarbons. Carbon, 2004, 42, 1057-1061.	5.4	36
210	Filamentous carbons as a support for heteropoly acid. Journal of Molecular Catalysis A, 2004, 211, 131-137.	4.8	23
211	Preparation of colloidal solutions of noble metals stabilized by polyoxometalates and supported catalysts based on these solutions. Kinetics and Catalysis, 2004, 45, 870-878.	0.3	12
212	New fluorinated carbon support for catalysts. Journal of Molecular Catalysis A, 2004, 217, 155-160.	4.8	9
213	Coprecipitated iron-containing catalysts (Fe-Al2O3, Fe-Co-Al2O3, Fe-Ni-Al2O3) for methane decomposition at moderate temperaturesl. Genesis of calcined and reduced catalysts. Applied Catalysis A: General, 2004, 268, 127-138.	2.2	70
214	Catalytic filamentous carbon as supports for nickel catalysts. Carbon, 2004, 42, 143-148.	5.4	53
215	Self-assembling carbon filament ropes formation. Carbon, 2004, 42, 1037-1042.	5.4	7
216	Gasification behavior of catalytic filamentous carbon. Carbon, 2004, 42, 2501-2507.	5.4	11

#	Article	IF	CITATIONS
217	The Formation of Clusters and Nanocrystals in Er-Implanted Hexagonal Silicon Carbide. Microscopy and Microanalysis, 2004, 10, 301-310.	0.2	6
218	Esterification of n-Butanol with Acetic Acid in the Presence of H3PW12O40Supported on Mesoporous Carbon Materials. Kinetics and Catalysis, 2003, 44, 778-787.	0.3	15
219	Title is missing!. Russian Journal of Electrochemistry, 2003, 39, 253-262.	0.3	2
220	Catalytic filamentous carbon. Carbon, 2003, 41, 1605-1615.	5.4	136
221	Structural properties of MBE grown Cu(In,Ga)S2 layers on Si. Journal of Physics and Chemistry of Solids, 2003, 64, 1491-1494.	1.9	10
222	Carbon capacious Ni-Cu-Al2O3 catalysts for high-temperature methane decomposition. Applied Catalysis A: General, 2003, 247, 51-63.	2.2	214
223	Enhanced Compositional Contrast in Imaging of Nanoprecipitates Buried in a Defective Crystal Using a Conventional TEM. Microscopy and Microanalysis, 2003, 9, 36-41.	0.2	22
224	Epitaxial Culn(1â^'x)GaxS2 on Si(111): A perfectly lattice-matched system for xâ‰^0.5. Applied Physics Letters, 2003, 83, 1563-1565.	1.5	5
225	Nucleation as Self-assembling Step of Carbon Deposit Formation on Metal Catalysts. AIP Conference Proceedings, 2003, , .	0.3	0
226	Lattice parameter measurement by CBED: Accuracy limited by the noise. Microscopy and Microanalysis, 2003, 9, 356-357.	0.2	0
227	Considerations on the accuracy of lattice parameters determined from HRTEM images. Microscopy and Microanalysis, 2003, 9, 166-167.	0.2	1
228	Defects in hexagonal SiC analyzed by Molecular Dynamics and HRTEM image simulations. Microscopy and Microanalysis, 2003, 9, 204-205.	0.2	0
229	Z-contrast imaging in a conventional TEM. Microscopy and Microanalysis, 2003, 9, 78-79.	0.2	2
230	Fluorination of Arc-Produced Carbon Material Containing Multiwall Nanotubes. Chemistry of Materials, 2002, 14, 1472-1476.	3.2	70
231	Fluorine Effect on the Structure and Electrical Transport of Arc-Produced Carbon Nanotubes. AIP Conference Proceedings, 2002, , .	0.3	2
232	Direct observation of defect-mediated cluster nucleation. Nature Materials, 2002, 1, 102-105.	13.3	97
233	The temperature dependence of the electrical resistivity and the negative magnetoresistance of carbon nanoparticles. Physics of the Solid State, 2002, 44, 487-489.	0.2	9
234	Gas-phase synthesis of nitrogen-containing carbon nanotubes and their electronic properties. Physics of the Solid State, 2002, 44, 652-655.	0.2	29

#	Article	IF	CITATIONS
235	TEM evidence for factors affecting the genesis of carbon species on bare and K-promoted Ni/MgO catalysts during the dry reforming of methane. Carbon, 2002, 40, 1063-1070.	5.4	71
236	Adsorption of H3PW12O40 by porous carbon materials. Russian Chemical Bulletin, 2002, 51, 243-248.	0.4	15
237	Title is missing!. Doklady Physical Chemistry, 2002, 386, 207-210.	0.2	5
238	Title is missing!. Kinetics and Catalysis, 2002, 43, 698-710.	0.3	3
239	Thermodynamic analysis of nucleation of carbon deposits on metal particles and its implications for the growth of carbon nanotubes. Physical Review B, 2001, 64, .	1.1	107
240	X-ray Emission Studies of the Valence Band of Nanodiamonds Annealed at Different Temperatures. Journal of Physical Chemistry A, 2001, 105, 9781-9787.	1.1	64
241	Evidence for 9R-SiC?. Microscopy and Microanalysis, 2001, 7, 368-369.	0.2	0
242	Evidence for 9R-SiC?. Microscopy and Microanalysis, 2001, 7, 368-369.	0.2	3
243	The structure of Si nanocrystals on SiC. Journal of Electron Microscopy, 2001, 50, 311-319.	0.9	10
244	Anisotropic properties of carbonaceous material produced in arc discharge. Applied Physics A: Materials Science and Processing, 2001, 72, 481-486.	1.1	25
245	Decomposition of Methane over Iron Catalysts at the Range of Moderate Temperatures: The Influence of Structure of the Catalytic Systems and the Reaction Conditions on the Yield of Carbon and Morphology of Carbon Filaments. Journal of Catalysis, 2001, 201, 183-197.	3.1	292
246	Electrical resistivity of graphitized ultra-disperse diamond and onion-like carbon. Chemical Physics Letters, 2001, 336, 397-404.	1.2	136
247	Analysis of Strain and Defect Formation of Low-Dimensional Structures in SiC. Materials Science Forum, 2001, 353-356, 259-262.	0.3	1
248	Fluorinated cage multiwall carbon nanoparticles. Chemical Physics Letters, 2000, 322, 231-236.	1.2	46
249	Catalytic synthesis of carbon nanostructures from polymer precursors. Journal of Molecular Catalysis A, 2000, 158, 301-307.	4.8	46
250	XPS and TEM study of new carbon material: N-containing catalytic filamentous carbon. Journal of Molecular Catalysis A, 2000, 158, 413-416.	4.8	25
251	Synthesis and study of palladium colloids and related catalysts. Journal of Molecular Catalysis A, 2000, 158, 461-465.	4.8	9
252	Platinum electrodeposits on glassy carbon: The formation mechanism, morphology, and adsorption properties. Russian Journal of Electrochemistry, 2000, 36, 741-751.	0.3	37

#	Article	IF	CITATIONS
253	Pd-Clusters on Carbon: Structure of Adsorbed PdCl ₂ Clusters and Interaction with Matrix. Materials Science Forum, 2000, 321-324, 1074-1077.	0.3	6
254	Aligned carbon nanotube films for cold cathode applications. Journal of Vacuum Science & Technology an Official Journal of the American Vacuum Society B, Microelectronics Processing and Phenomena, 2000, 18, 1059.	1.6	56
255	Illusion of New Polytypes. Materials Science Forum, 2000, 338-342, 533-536.	0.3	0
256	Kinetics of the graphitization of dispersed diamonds at "low―temperatures. Journal of Applied Physics, 2000, 88, 4380.	1.1	162
257	Thin film cold cathode from nanostructured carbon. , 1999, , .		0
258	A transmission electron microscopy investigation of SiC films grown on SiC substrates by solid-source molecular beam epitaxy. Journal of Materials Research, 1999, 14, 3226-3236.	1.2	5
259	Control of the size and photochemical properties of Q-CdS particles attached to the inner and/or outer surface of the lecithin vesicle bilayer membrane by the nature of its precursors. Journal of Photochemistry and Photobiology A: Chemistry, 1999, 125, 127-134.	2.0	11
260	On the peculiarities of bright/dark contrast in HRTEM images of SiC polytypes. Ultramicroscopy, 1999, 76, 21-37.	0.8	15
261	Role of the curvature of atomic layers in electron field emission from graphitic nanostructured carbon. JETP Letters, 1999, 69, 411-417.	0.4	32
262	Theoretical study of the formation of closed curved graphite-like structures during annealing of diamond surface. Journal of Applied Physics, 1999, 86, 863-870.	1.1	175
263	Origin of Threefold Periodicity in High-Resolution Transmission Electron Microscopy Images of Thin Film Cubic SiC. Microscopy and Microanalysis, 1999, 5, 420-427.	0.2	11
264	Oriented Carbon Nanotube Growth for Field Emission Applications. Materials Research Society Symposia Proceedings, 1999, 558, 111.	0.1	1
265	Raman identification of onion-like carbon. Carbon, 1998, 36, 821-826.	5.4	205
266	Closed curved graphite-like structures formation on micron-size diamond. Chemical Physics Letters, 1998, 289, 353-360.	1.2	56
267	Observation of 3-Fold Periodicity in 3C-SiC Layers Grown by MBE. Materials Science Forum, 1998, 264-268, 259-264.	0.3	3
268	On the nature of the interaction of H2PdCl4 with the surface of graphite-like carbon materials. Carbon, 1997, 35, 73-82.	5.4	78
269	Systematic Study of Metal Particles (Pt, Ni) Contrast on Amorphous Support (Silica) Using Multislice. , 1997, , 371-374.		0
270	Structure of polynuclear palladium(II) hydroxocomplexes and the mechanism of their adsorption by carbon materials. Russian Chemical Bulletin, 1996, 45, 1296-1302.	0.4	12

#	Article	IF	CITATIONS
271	Long- and short-distance ordering of the metal cores of giant Pd clusters. Journal of Crystal Growth, 1996, 163, 377-387.	0.7	44
272	Chemical and morphological characterization of a direct methanol fuel cell based on a quaternary Pt-Ru-Sn-W/C anode. Journal of Applied Electrochemistry, 1996, 26, 959.	1.5	57
273	Vacancy Ordering in γ-Fe2O3: Synchrotron X-ray Powder Diffraction and High-Resolution Electron Microscopy Studies. Journal of Applied Crystallography, 1995, 28, 141-145.	1.9	147
274	Structure of polynuclear palladium(ii) hydroxocomplexes formed upon alkaline hydrolysis of palladium(ii) chloride complexes. Russian Chemical Bulletin, 1995, 44, 1822-1826.	0.4	22
275	Formation of carbon particles of onion structure from ultradisperse diamond. Combustion, Explosion and Shock Waves, 1994, 30, 131-132.	0.3	3
276	Effect of explosion conditions on the structure of detonation soots: Ultradisperse diamond and onion carbon. Carbon, 1994, 32, 873-882.	5.4	185
277	Onion-like carbon from ultra-disperse diamond. Chemical Physics Letters, 1994, 222, 343-348.	1.2	610
278	Study of Onion-Like Carbon (OLC) Formation from Ultra Disperse Diamond (UDD). Materials Research Society Symposia Proceedings, 1994, 359, 105.	0.1	13
279	Magnesia-Supported Nickel Catalysts. Journal of Catalysis, 1993, 141, 34-47.	3.1	87
280	Formation of diamond from the liquid phase of carbon. Combustion, Explosion and Shock Waves, 1993, 29, 542-544.	0.3	22
281	Highly dispersed platinum honeycomb reforming catalysts: Sintering behavior and activity. Reaction Kinetics and Catalysis Letters, 1992, 48, 315-323.	0.6	1
282	Gas-phase hydroformylation of propylene on Ru/SiO2 catalysts. Reaction Kinetics and Catalysis Letters, 1991, 44, 139-146.	0.6	8
283	Study of ultradispersed diamond powders obtained using explosion energy. Carbon, 1991, 29, 665-668.	5.4	122
284	Influence of carbon support pretreatment on properties of Pd/C catalysts. Reaction Kinetics and Catalysis Letters, 1990, 41, 211-216.	0.6	12
285	Preparation of palladium catalysts via thermal decomposition of supported Pd(O) complexes. Reaction Kinetics and Catalysis Letters, 1989, 38, 109-114.	0.6	4
286	Acidoligand substitution in large palladium clusters. Bulletin of the Academy of Sciences of the USSR Division of Chemical Science, 1989, 38, 762-766.	0.0	0
287	Palladium catalysts on carbon supports 2. Description of the adsorption equilibria of Pd(II) in the H2PdCl4-HCl-carbon support system. Bulletin of the Academy of Sciences of the USSR Division of Chemical Science, 1989, 38, 1792-1796.	0.0	0
288	Giant palladium clusters as catalysts of oxidative reactions of olefins and alcohols. Journal of Molecular Catalysis, 1989, 53, 315-348.	1.2	183

#	Article	IF	CITATIONS
289	Effect of dispersion of supported palladium on its electronic and catalytic properties in the hydrogenation of vinylacetylene. Applied Catalysis, 1988, 42, 131-141.	1.1	78
290	New carbon material as support for catalysts. Reaction Kinetics and Catalysis Letters, 1987, 33, 435-440.	0.6	163
291	Giant palladium cluster with a face-centered-cubic metal framework lattice. Bulletin of the Academy of Sciences of the USSR Division of Chemical Science, 1986, 35, 237-237.	0.0	1
292	Nanocomposite Coatings Produced by Friction Cladding. Advanced Materials Research, 0, 59, 220-224.	0.3	0